Particle reinforced composites' elastic properties retrieval by aid of laser generated ultrasound waves

D. LUCA MOTOC[a*], S. FERRANDIZ BOU[b], A. POP[c]
[a]*Department of Materials Science, Transilvania University, 500036 Brasov, Romania*
[b]*Department of Mechanical and Materials Engineering, Polytechnic University of Valencia, Spain*
[c]*Department of Mechatronics, University of Oradea, 410087 Oradea, Romania*

The paper aims to present a comparative analysis on numerical approaches carried on particle reinforced polymer composites viscoelastic properties' recovery procedure deployed to assist a laser generated ultrasound experimental configuration. A laser ultrasound technique was used to record the displacement fields within the composite specimens. A numerical procedure developed with Laser Group from University of Bordeaux is assisting the elastic coefficients' recovery process from the recorded signal. Corresponding theoretical displacements and stress/strain fields were simulated by finite-element method and further compared to the experimental signals. Agreement between the experimentally recorded signals and theoretical predictions is being found.

(Received April 9, 2015; accepted June 24, 2015)

Keywords: Polymer composites, Elastic properties, Laser ultrasound, Ablation mode

1. Introduction

Ultrasonic material testing has been widely used for decades due to its versatility and handling facilities. Numerous techniques emerged and proved viable in assisting the material characterization and inspection. Noteworthy is the last review of Chimenti (2014) on air-coupled ultrasonic material characterization devices, techniques and applications [1]. In addition, the emphasis is on how to overcome the limitation inherent to these experimental configurations, followed by carefully examination of the outstanding work of Hosten (1998, 2008) and his collaborators [2-3].

Laser generated ultrasound emerged as one of the air-coupled material characterization methods. A laser source operated in the thermo-elastic regime generates ultrasound waves through thermal expansion while used at the low-power level. Opposite, at the high-power level, the laser source operates in the ablation regime and gives rise to vaporization of a small amount of material.

Numerous researchers tackled the issue of ultrasound wave generation from a laser source by fully operating it on the ablative and thermo-elastic regime. Viewed as one of the major contributors in the field of laser generated ultrasound, Karabuthov (1998, 2000, and 2010) is continuously surprising the scientific world. Contributions are targeting the use of laser generated ultrasound to recover the elastic coefficients in unidirectional graphite-epoxy composites or layered materials [4-6].

Next, all references contain theoretical approaches in addition to the experimental recorded signals. Agreements between experimental recorded and theoretical reported values are found.

Technical difficulties associated with the recording of ultrasonic field are overcome by use of high sensitive optical detectors and proper material recovery techniques. An understanding of generated wave propagation from different distributed (i.e. point, linear) sources is advisable before commencing the properties' recovery procedure, as suggested by Pan et al. (2006) or Audoin (2001, 2008) in their sharing contributions [7-9].

Thereto, noteworthy is to underline the approach of sensitivity issue while tackling the recovery of elastic coefficients from laser generated ultrasound waves within polymer composites with string anisotropy [10-11]. Since the phase or group velocities of ultrasonic bulk waves are deployed within an inverse procedure, the latter can examined by extensive simulations [12-14]. These are illustrating the effect of input data distortion and incompleteness while converting the velocities type.

Finite-element method (FEM) is being used due to its versatility and flexibility in modelling complicated geometries and loading conditions. Several contributions are tackling the issue of FEM usage to simulate the distribution of displacement and stress fields generated within an isotropic or viscoelastic specimen by a dynamic thermal source resembling the laser generated ultrasound [15-16]. The input data values account the finite spatial and temporal shape of the laser pulse, optical penetration and temperature dependence of material properties.

The paper aims to approach the issue of laser ultrasound pulses from a source running in ablative mode, linearly distributed over the surface of an epoxy based composite specimens. The recovered elastic coefficients using a numerical procedure developed within the Laser Group from University of Bordeaux are further used as input data into an FEM based environment.

In addition, the temporal and spatial range of the linearly distributed laser source was deployed to enable

stress and strain field contours during the transient thermal analysis carried out.

Debate on similarities between finite element method aided simulated displacements and experimentally recorded is being approached and closely investigated. The primary aim is to demonstrate the feasibility of FEM aided simulation usage in laser ultrasonic non-destructive material characterization.

2. Materials and methods

2.1. Materials

By embedding different volume fractions of alumina particles within an epoxy resin using a hot compressing technique enabled specimens' manufacturing. The polymer resin is available under the Hexcel MY 750 trademark while the hardener under HY 907, from Hexcel Corporation (Dublin, CA). The polymer matrix can withstand high temperatures like those generated by a laser source. The mixture was pressed at specimens' final dimensions of 100x8 mm^2 as cylindrical shapes.

Composite specimens differ in terms of fillers' volume fraction point of view. They are labelled relative to filler content, as following: sample 1 – 45%, sample 2 – 40% and sample 3 – 35%, respectively.

Table 1 lists the polymer resin's properties as they were further used as input in the simulation environment.

Table 1. Polymer matrix properties used in simulation

Physical properties	
Young's modulus [GPa]	3
Shear modulus [GPa]	1.09
Poisson's ratio	0.38
Glass transition temperature [°C]	160

2.2 Experimental technique

A Nd:YAG laser source, emitting at 1064 nm, was used to generate the ultrasonic waves in short pulses having 20 ns duration. The medium power output is typically ranging from 10 to 250 mJ per pulse. The collimated optical beam is focused onto the composite specimen by means of a cylindrical lens. The latter enable to generate a line source dimension for the ultrasonic waves within the composite specimens. Ablation occurs at the side facing the laser source, marking it slightly, as can be seen in Fig. 1.

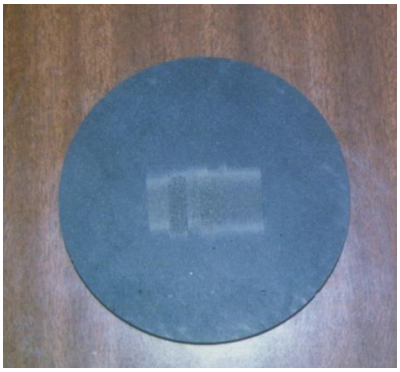

Fig. 1 Laser ablation signature on specimens' surface

From a conceptual perspective, this can be represented as a force normal to the surface of the specimen. Furthermore, this type of source generates a high-amplitude bulk longitudinal wave on the receiver side.

Detection is carried out by aid of a Mach-Zender laser interferometer probe, heterodyne type. The bandwidth extended up to 10 MHz. The reflectance of the specimens' surface does not enable a proper use of the heterodyne probe, requiring thus the use of a thin aluminium foil to increase the signal to noise ratio.

The signals were further amplified and sent to a computer connected to the transducer for further data processing.

3. FEM modelling of transient response

A coupled transient thermo-dynamical analysis enabled laser generated ultrasound problem approach within ANSYS 12.0 simulation environment [20]. First, a thermal element was used to simulate the thermal field. Then, the stress and displacement fields are simulated by replacing the above with a structural element (VISCO 88) that accounts for the viscous-elastic behaviour of the polymer matrix.

The initial and boundary conditions for modelling are set as follows: the initial temperature is assumed to be the ambient temperature. The load is considered linearly distributed over 25 mm, as focused by the cylindrical lens. Moreover, heat convection and thermal radiation are neglected.

The laser energy is 18 mJ and pulse rise time at the specimen surface is taken to be 20 ns. The maxim temperature achieved for a pulse width of 20 ns is about 618 °C, high enough to get ablation on specimen surface. Temporal and spatial resolution of the finite model is critical to the convergence of the numerical results [15].

4. Results and discussions

This section contains explanations on stiffness coefficients' recovery procedures followed by a discussion on simulation results gathered from FEM analysis.

The composite specimens' stiffness coefficients are recovered in two steps: (a) processing of group velocities from signals collected on the receiver side; (b) use of a numerical scheme developed to enable stiffness coefficients' recovery.

4.1 Elastic coefficients from measurements

The numerical recovery of the elastic coefficients from experimental velocities and amplitude of bulk modes from the laser source is already ascribed in reference papers [2, 17-19]. The elastic stiffness coefficients C_{ij} are defined in an axis system such as that direction 1 is the normal to the specimen and directions 2 and 3 are lying in the plane.

In the particle reinforced viscoelastic specimens, like those herein, two main elastic coefficients must be identified – C_{11} and C_{12}, the third being estimated from a dependency between the other ones.

The well-known elastic stiffness matrix for isotropic media in Voigt notation is:

$$C_{ij} = \begin{bmatrix} C_{11} & C_{12} & C_{12} & 0 & 0 & 0 \\ 0 & C_{11} & C_{12} & 0 & 0 & 0 \\ 0 & 0 & C_{11} & 0 & 0 & 0 \\ 0 & 0 & 0 & C_{44} & 0 & 0 \\ 0 & 0 & 0 & 0 & C_{44} & 0 \\ 0 & 0 & 0 & 0 & 0 & C_{44} \end{bmatrix} \quad (1)$$

Since in isotropic media only two waves are propagating through, longitudinal and shear, their velocities may be related to the material's properties.

The relationships between longitudinal and shear velocities and elastic coefficients in isotropic media are as follows:

$$v_T = \sqrt{\frac{C_{11} - C_{12}}{2\rho}} \quad (1)$$

$$v_L = \sqrt{\frac{C_{11}}{\rho}} \quad (2)$$

where ρ is the density of polymer based composite material and C_{ij} the stiffness coefficients from above.

From numerical scheme implementation, the stiffness coefficients are derived employing the Christofell equations that related each recorded velocity phase to these [3-4].

On the other hand, stiffness coefficients recovered from group velocities is not straightforward as previous. Since there are no equations available, several methods for solving this inverse problem exist in literature [18].

In connection with above, the algorithm proposed by Deschamps and Bescond departs from the Cagniard-de Hoop method employed usually to relate the proposed change in variable and solving the expression of Christofell afterward. They identified a simple relationship between the group velocity and waves' time of arrival and deployed further.

In Table 2 is listed the experimental values retrieved after using an optimized numerical recovery procedure as described above.

The values are consistent with the fillers' volume fraction embedded within the polymer composite. Small discrepancies exist between the recovered elastic coefficients in directions 2 and 3. These discrepancies are neglected and can be regarded to the manufacturing conditions and sensitivity of the experimental devices. Nevertheless, these characterize the quality of stiffness coefficients recovery process from group velocity data.

The stiffness coefficient C_{11} is recovered from the longitudinal wave velocity propagating in the direction of epicentre direction, whereas C_{12} from velocities of waves travelling in transversal direction. Noteworthy, the recovered values are ascribed to the room temperature recorded signals since they depend upon temperature.

Table 2. Elastic coefficients recovered from measurements at

Sample	*Elastic coefficients*	
	C_{11}	C_{12}
Sample 1	22.3 ± 0.85	6.52 ± 0.3
Sample 2	21.6 ± 0.63	5.75 ± 0.3
Sample 3	20.7 ± 0.48	6.5 ± 0.4

4.2 FEM simulation of stress/displacements fields

A numerical recovery procedure and modelling of laser generated ultrasound is employed to aid elastic coefficients' retrieval of polymer based composite specimens. The temporal shape of the laser pulses is accounted, also.

In Fig. 2 and Fig. 3 is being plotted the displacements' field recorded along the main direction of laser pulse loading within samples 1 and 3. These were simulated to cover the entire temporal range between incidence and emergence on the receiver side.

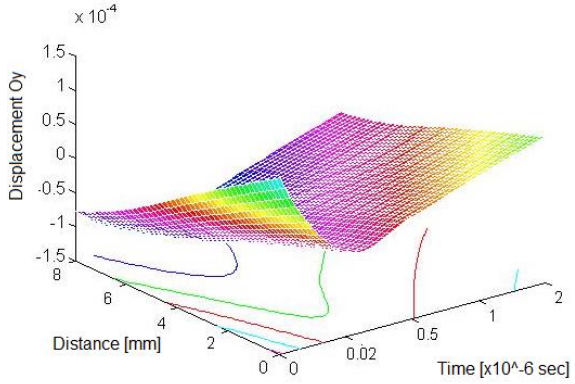

Fig. 2 FEM simulated displacement field from sample 1

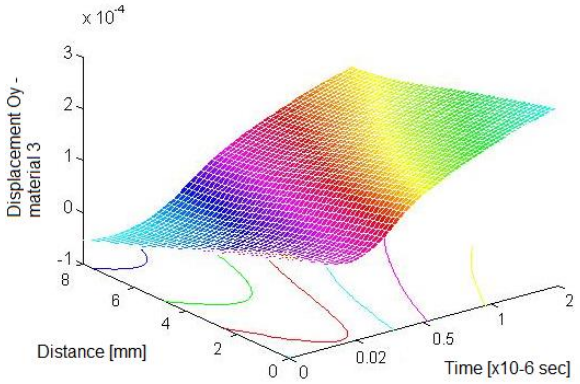

Fig. 3 FEM simulated displacement field from sample 3

A closer look to the above variations, both in time and penetration distance of the laser pulses reveal their consistency with the experimental recorded displacement field.

In all specimens, a negative spike is recorded within 20 ns associated to the extern load temporal range. The same trend is being recorded experimentally along the epicentre as a distinguished feature in the longitudinal component of the ultrasonic wave front. This is associated to the thermal stress generated by incidence of the laser pulse that causes surface heating and expansion.

The magnitude of this spike is strongly affected by the mass evaporated during the pulse interaction with sample's surface.

In Fig. 4 and Fig. 5 is represented the total strain fields within samples 1 and 2 along their thickness and within temporal range set to cover pulse propagation. In Fig. 6 is being

The following graphical representations and contour plots reflect the loading conditions, both temporal and thermal. Noteworthy, these follow the vertical and horizontal distribution of the external load that can be translated in terms of ultrasonic wave as longitudinal and transversal/surface propagation modes.

As previously described, thermal stresses are generated within the sample by laser heating. Fig. 6 captures this effect, including also the dynamic response due to a very short temporal range of the laser pulse. Both elastic and thermal stress develops nearby the sample surface and propagates downward.

Plot from Fig. 7 better depict the influence of the precursor on the in-plane stress field while its amplitude increases with the optical penetration depth. The contours of the in-plane stress indicate that it is compressive with a maximum recorded at 20 ns from load action and move further inside the sample's thickness.

The similar contour tendencies can be seen in the in-plane stress elastic field variation, both time and specimen distance from source side. This is outlined in Fig. 8.

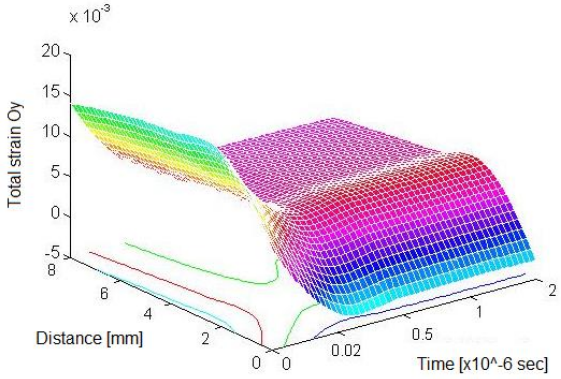

Fig. 4 Total strain fields generated within sample 1

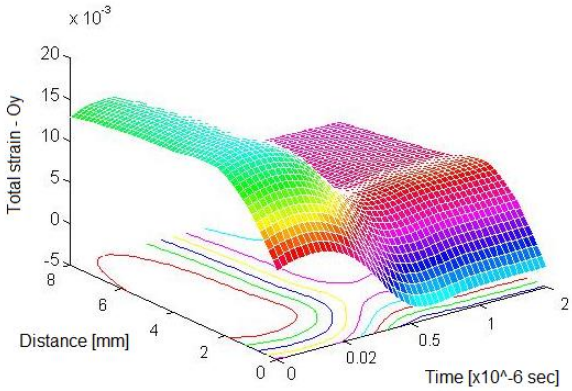

Fig. 5 Total strain fields generated within sample 2

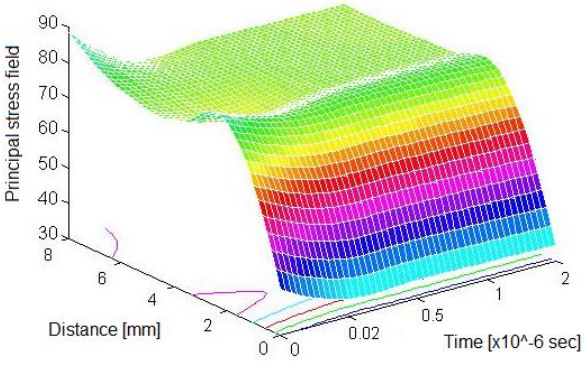

Fig. 6 Total stress fields generated within sample 1

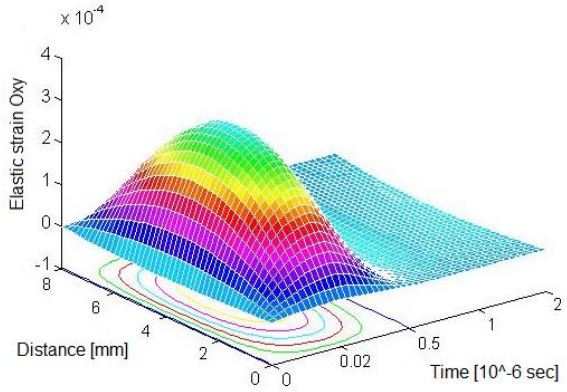

Fig. 7 In-plane elastic strain field within sample 1

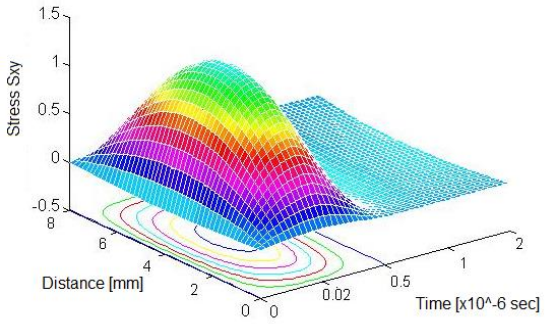

Fig. 6 In-plane elastic stress field within sample 1

In Fig. 9 and Fig. 10 is being plotted the displacement fields recorded in the epicenter direction at time arrival corresponding to the incidence at the laser source side, respectively at the detection side.

These resemble the experimentally recorded signals especially at the incidence since again the negative spike can be underlined.

Since thermal strain exists along with elastic ones due to both transient and inherent nature of the laser source, in Fig. 11 is represented the count plots of these fields along epicenter direction in sample 1.

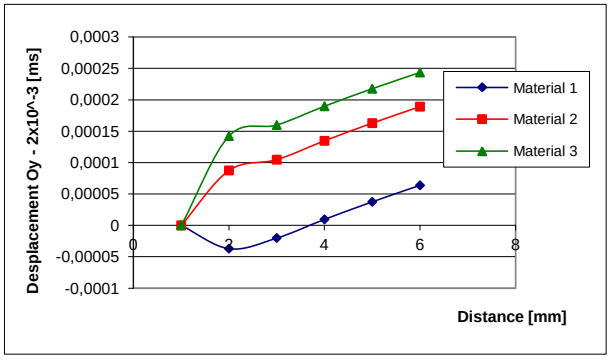

Fig. 9 Displacement field in epicenter direction recorded at 2 µs

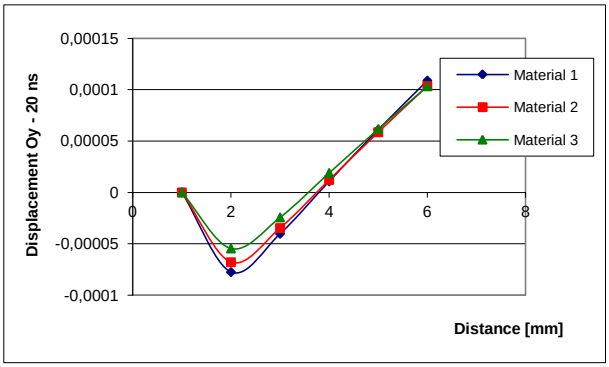

Fig. 10 Displacement field in epicenter direction recorded at 20 ns

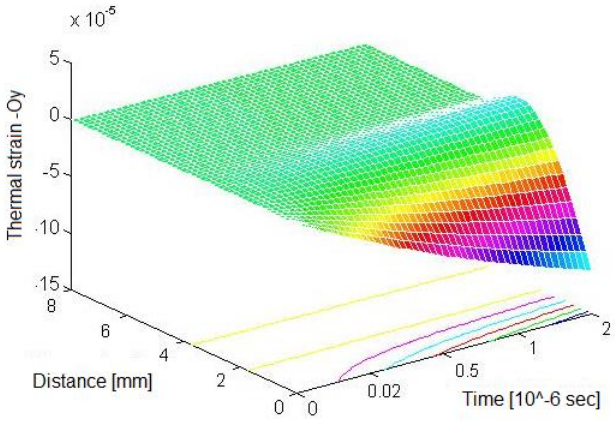

Fig. 11 Thermal strain field within sample 1 along epicenter direction

Noteworthy is the variation of the strain field that has the same trend in all composite samples. This is very high nearby the surface and turns to diminishing on the receiver side. The same hold in the experimental side for high-amplitude incidence pulses of laser source.

Furthermore, as the pulses depart from the incidence side, a relaxation process occurs. This can be sized in the strain field variation, irrespective of elastic or thermal ones.

Regarding all simulation results, the specimen shape does not influence the stress/strain field in epicenter direction. Contrary, in practice this gives rise to other types of waves hat should be further identified and quantified.

5. Conclusions

The issue of laser generated ultrasound still captures researchers' attention due to its feasibility in enabling material properties' recovery from experimental recorded displacement fields.

A circular approach has been deployed herein to enable comparison between related experimentally signals and FEM simulated stress/strain or displacement variations.

On the other hand, optimized numerical recovery procedures of properties in isotropic/anisotropic materials are well developed and successfully used by several research groups. In this case, one particular developed is used for particle epoxy reinforced composites elastic coefficients' recovery proven different volume fraction of constitutive.

Despite the advent of FEM deployment on solving thermal transient propagation like the herein approached subject, a closer attention should be pay on capturing the entire coupled effects due to the loading conditions (i.e. temporal range, distribution, incidence to surface, etc.).

In relation with above, it's noteworthy for mention the breakdown in encompassing the overall effects generated by wave propagation, longitudinally and transversally. This can be related to the shortage in computer resources and abilities in running incrementally time/space distributed loading conditions.

Acknowledgment

The corresponding author gratefully acknowledges the financial assistance from Erasmus program that enabled and supported the internship with Laboratoire of Mechanique-Physique, Universite Bordeaux, France.

References

[1] D. E. Chimenti, Ultrasonics **54** (7), 1804 (2014).
[2] Bernard Hosten, Ultrasonics **30** (6), 365 (1992).
[3] B. Hosten, M. Castaings, Composites Part A: Applied Science and Manufacturing **39** (6), 1054 (2008).
[4] A. A. Karabutov, I. M. Kershtein, I. M. Pelivanov, N. B. Podymova, Mechanics of Composite Materials **34**(6), 575 (1998).
[5] A. A. Karabutov, Jr., A. A. Karabutov, O. A. Sapozhnikov, Phys. Wave Phen. **18**(4), 297 (2010).
[6] AA Karabutov, IM Pelivanov, NB Podymova, Mechanics of composite materials **36** (6), 497 (2000).
[7] S. Guilbaud, B. Audoin, Composites Science and Technology **61** (3), 433 (2001).
[8] Y. Pan, C. Rossignol, B. Audoin, N. Chigarev, Ultrasonics **44, Supplement** (0), e1249 (2006).
[9] B. Audoin, Ultrasonics **40**(1–8), 735 (2002).
[10] Hanuš Seiner, Michal Landa, Ultrasonics **43**(4), 253 (2005).
[11] Victor V. Kozhushko Peter Hess, Journal of Applied Physics **103**(12), 124902 (2008).
[12] V. Kalkis, M. Kalnins, Ya Zitsans, Mechanics of Composite Materials **33**(3), 282 (1997).
[13] Jean-Yves Chatellier, Maurice Touratier, The Journal of the Acoustical Society of America **83**(1), 109 (1988).
[14] Zi-quan Li, Xiao-rong Zhang, Shu-yi Zhang, Zhong-hua Shen, Composites Science and Technology **61**(10), 1457 (2001).
[15] Jijun Wang, Zhonghua Shen, Baiqiang Xu, Xiaowu Ni, Jianfei Guan, and Jian Lu, Optics & Laser Technology **39**(4), 806 (2007).
[16] Ling Yuan, Yifei Shi, Zhonghua Shen, Xiaowu Ni, Optics & Laser Technology **40**(2), 325 (2008).
[17] J. D. Aussel and J. P. Monchalin, Ultrasonics **27**(3), 165 (1989).
[18] M. Deschamps, C. Bescond, Ultrasonics **33**(3), 205 (1995).
[19] B. Audoin, C. Bescond, J Nondestruct Eval **16**(2), 91 (1997).
[20] D. Luca Motoc, Contribution to the study of stress state and physical properties of materials using nondestructive testing methods, PhD thesis (2002).

*Corresponding author: danaluca@unitbv.ro